Frequency Response Range of Semiactive Magnetorheological Tuned Mass Dampers

Cory W. Lindh, Simon Laflamme and Jerome J. Connor
Dept. of Civil and Env. Eng., MIT, 77 Mass. ave., Cambridge, MA 02139

ABSTRACT

The effective frequency range of a controlled semiactive tuned mass damper equipped with a magnetorheological variable damping device is assessed. The phenomenological model for the magnetorheological damper and a sliding mode controller with a clipped-optimal control algorithm are used to simulate the semiactive tuned mass damper. Through numerical techniques, the responses of single degree of freedom and multi degree of freedom structures are simulated for an optimally tuned passive tuned mass damper, the semiactive sheme, and an ideal active mass driver. Development of the corresponding transfer functions demonstrates greater response mitigation around the tuned frequency and a wider band of attenuated frequencies for the controlled semiactive system, except for a small region at the resonance frequency. The control scheme is also capable of reaching higher modes. The capabilities and limitations of controlled magnetorheological dampers in tuned mass damper applications are to be further investigated to quantitatively assess the frequency reachability of the structural control scheme.

EXTENDED ABSTRACT

1.0 INTRODUCTION

The mitigation of structural response under dynamic loading has been approached through a variety of damping techniques. Undesirable vibrations due to winds or earthquakes must be mitigated to protect the structure and to ensure safety and comfort of its occupants. One reliable vibration control device is the tuned mass damper (TMD), consisting of a mass, a damper, and a spring, the properties of which are generally optimized to respond to the resonant frequency of the structural fundamental mode. Though effective for excitations of this kind, the primary limitation of the TMD is its narrow band of frequency suppression (about 15% of the tuned frequency), as determined by its fixed parameters [1]. Consequently, it is desirable to improve upon the TMD passive control capabilities by using either active of semi-active control to expand its effective frequency range.

Active control for TMDs has been widely studied and is perhaps one of the most accepted active control schemes in civil structures [2-4]. Active TMDs have notable advantages over passive TMDs, including the capability to efficiently reach most of the frequency domain and to perform well even if tuning has been performed with system uncertainties. Nevertheless, their limitation is the reliability on an external power source that could be unavailable during extraordinary natural hazards. Hybrid and semi-active TMD systems have been suggested, which offer the advantage of low power consumption. Kim and Adeli [5] proposed a hybrid damper-tuned liquid damper system. The effectiveness of a semiactive TMD (STMD) with idealized variable damping has been demonstrated by Pinkaew and Fujino [6] through a simulated comparison with passive TMDs. A numerical optimization method for STMDs was recommended by Lee, *et al.* [7] and applied to a benchmark 10 story shear structure. Lin and Loh [8] proposed an STMD consisting of a magnetorheological (MR) damper attached to the TMD. Their numerical analysis demonstrated the effectiveness in the MR-damper STMD in greatly improving the control efficiency of the passive TMD. Ji, *et al.* [9] explored various control algorithms for the MR-STMD, identifying the best results for various combinations of dynamic loads.

The use of MR damper in hybrid systems, such as the STMD, is promising. MR dampers provide reliable performance with low power consumption. For instance, they can provide a reactive force up to 200 kN for a 50 W power input [10]. They can therefore be plugged on batteries and be still operating upon a general power failure. Many control algorithms have been studied in the aforementioned papers to control STMDs. However, to the best of our knowledge, none have addressed the frequency and modal capability of such systems, whose performance is intuitively located between the passive and the active TMD schemes. This research studies the frequency and modal capability of a TMD system equipped with an MR damper and compares its performance with passive and active systems to mitigate a variety of excitations.

2.0 METHOD

2.1 Tuned-Mass Dampers

The first tuned mass damper system was proposed by Frahm in 1909 to reduce mechanical vibrations [11]. Its structural applicability was first explored by Den Hartog in 1940, whose analysis of a single-degree-of-freedom (SDOF) system without damping provided analytical solutions for optimizing TMD parameters [12]. Numerical adaptations of Hartog's method have included the use of multiple tuned mass dampers in a single structure and optimization of tuned mass damper parameters for multiple-degree-of-freedom (MDOF) structures [7,13].

The design of passive TMDs is based on limiting the response of a structure at resonance. Generally, the fundamental mode is of greatest significance. By performing a modal decomposition, the mode of interest is treated as an SDOF. Appending a tuned mass to an undamped structure leads to the following equations of motion:

$$\begin{aligned} m_d(\ddot{u}_d + \ddot{u} + \ddot{u}_g) &= p(t) - c_d\dot{u}_d - k_d u_d \\ m(\ddot{u} + \ddot{u}_g) &= p(t) - ku + c_d\dot{u}_d + k_d u_d \end{aligned} \tag{1}$$

where u_g is the ground displacement under earthquake excitation, u is the structure's relative displacement, u_d is the relative displacement of the tuned mass, $p(t)$ is any dynamic loading, and m, k, m_d, k_d, and c_d are the structural properties of the building and TMD, respectively. TMD parameters are selected to minimize the response of the structure due to dynamic loading. Optimization leads to the following TMD design parameters:

$$\sqrt{\frac{k_d}{m_d}} = \frac{\sqrt{1 - 0.5\bar{m}}}{1 + \bar{m}}\sqrt{\frac{k}{m}} \tag{2}$$

where $\bar{m}$ is the mass ratio, m_d/m. For optimally-tuned passive TMDs, the damping effect can only be improved by increasing the mass ratio, which brings inherit weight and space limitations in civil structures.

2.2 Magnetorheological Dampers

Magnetorheological (MR) dampers are variable dampers made up of a rheological fluid whose properties can be altered through the application of an external magnetic field. The distinguishing characteristic of the MR fluid is it ability to reversibly change from a free-flowing, linear viscous fluid to a semisolid with a controllable yield strength in milliseconds once the magnetic field has been applied. The fluid is made of polarizable and magnetizable particles that line up upon magnetic excitation, thus allowing for this sudden change in viscosity [10].

Correctly modeling MR dampers has proved challenging due to hysteretic behavior and the stiction and shear thinning effects of the rheological fluid. Several mathematical and non-mathematical models have been proposed in the literature, among which is the phenomenological model proposed by Spencer *et al.* [14]. Their model is based on Bouc-Wen hysteresis and takes into account the stiction and shear thinning phenomena. The mechanical idealization of this model is shown to the right in Figure 1, with the hysteric behavior of the MR damper modeled by an evolutionary variable.

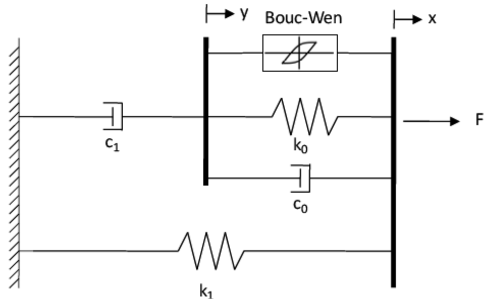

Figure 1: Phenomenological Model

The equations governing the phenomenological model are given below. This model is used for the simulation in the study.

$$f = c_1\dot{y} + k_1(x - x_0) \tag{3}$$
$$\dot{z} = -\gamma|\dot{x} - \dot{y}|z|z|^{n-1} - \beta(\dot{x} - \dot{y})|z|^n + A(\dot{x} - \dot{y})$$
$$\dot{y} = (c_0 + c_1)^{-1}\left(\alpha z + c_0\dot{x} + k_0(x - y)\right)$$

where f is the resulting force, $k_0, k_1, \beta, \gamma, A,$ and n are constants, z is an evolutionary variable, and $\alpha, c_0,$ and c_1 are voltage-dependent, defined by:

$$\alpha = \alpha_a + \alpha_b w \tag{4}$$
$$c_0 = c_{0a} + c_{0b} w$$
$$c_1 = c_{1a} + c_{1b} w$$
$$\dot{w} = -\eta(w - v)$$

where $\alpha_a, \alpha_b, c_{0a}, c_{0b}, c_{1a}, c_{1b},$ and η are constants, v is the applied voltage, and w is the actual voltage.

2.3 Simulation

In the following numerical examples, an MR-STMD system is simulated that uses the phenomenological model of the MR-damper on a SDOF. State-space numerical integration with a 1000 N capacity prototype MR damper was used to simulate the passive and controlled responses of structures equipped with a TMD. The first numerical model is of a SDOF system with a mass m = 1000 kg, a stiffness k = 15000 N/m, 1% damping, $\overline{m} = .01$, and optimized TMD stiffness. The structure is assumed to start at rest and is exposed to sinusoidal loading with frequencies sweeping from 0 to 50 rad/s.

A preliminary simulation is also performed on a 3 DOF shear building with $m_1 = m_2 = m_3 =$ 1500 kg, $k_1 = k_2 = k =$ 2100 kN/m, damping matrix C = 1% modal damping, $m_{TMD} = m_1/10$, and m_{TMD} = 36.4 kN/m.

Work to date shows the efficacy of the MR-damper STMD in mitigating the structural response to a wider range of frequencies than is accessible by passive TMDs. Results are to be extended to multi-degree-of-freedom (MDOF) systems to investigate the applicability of an MR-damper in mitigating frequencies in the range of a secondary resonance frequency. The authors will further compare the results to an active mass driver (AMD), consisting of an ideal actuator and a TMD. Through simulations of MR-TMDs on variously-sized structures, the authors seek to show that an MR-equipped STMD can harness the same frequency-range capabilities as TMDs in a more efficient form, and moreover covers a wider spectrum.

2.3.1 Controller

A sliding mode controller is implemented to analyze its effectiveness and to compare STMD results with passive TMDs and AMDs. The sliding mode controller has the capability to account for various uncertainties, among which the uncertainty on external excitation, but ideal knowledge will be assumed for comparison purposes. The controller used to control the STMD is not the focus of this study, and therefore the controller proposed by Adhikari and Yamaguchi [15] is utilized, and augmented by a clipped-optimal control algorithm [16] to select the voltage input.

The control law, given no uncertainties, is given by:

$$f_{req} = -\left(PB_f\right)^{-1}[PAX + PHf] \tag{5}$$

where $X \in R^{1x2n}$ is the state vector consisting of displacements and velocities, $H \in R^{2nx1}$ is the external force influence vector, f is the external force, $P \in R^{kx2n}$ is a user-defined matrix, *n* is the number of degree of freedom, *k* is the number of force input, $A \in R^{2nx2n}$ and $B_f \in R^{2nx1}$. These can be expressed as:

$$A = \begin{bmatrix} 0_{nxn} & I_{nxn} \\ -M^{-1}K & -M^{-1}C \end{bmatrix} \tag{6}$$
$$B_f = [0 \ \cdots \ 0_n \ diag(M^{-1})]'$$

where *M, C,* and *K* are the mass, damping, and stiffness matrices respectively. *P* is selected to be a weighted sum of the system states to define the sliding surface *S*:

$$S = PX \tag{7}$$

The technique to design matrix *P* is defined in Utkin and Young [17]. The target sliding surface is *S = 0*. Once the force is selected from the control law, a clipped-optimal algorithm will command a voltage to be inputted in the MR damper. In this algorithm, the applied voltage is maximum if the required force is higher than the actual damper force and of the same sign; it is set to zero otherwise. The clipped-optimal algorithm has shown good performance in the literature [18-19].

2.3.2 Simulated Models

The control algorithm was applied to TMD through numerical integration of the state-space formulation of the equations of motion:

$$\dot{X} = AX + B_f f + B_g a_g + B_p p \tag{8}$$

with:

$$B_g = [0 \ \cdots \ 0_n \ -1 \ \ldots \ -1_n]'$$
$$B_p = B_f$$

In the present case, $f = f_{MR}(t)$, the force outputted by the magnetorheological damper as given by the phenomenological model. This output is a function of the relative displacements and velocities of the two masses, as well as the voltage applied to the MR damper.

2.4 Preliminary Results

This numerical simulation was performed for the SDOF free vibration, the passive optimized TMD, the passive TMD with accompanying MR damper, and the controlled MR-TMD. The frequency response *H(ω)* is plotted below in Fig. 2.

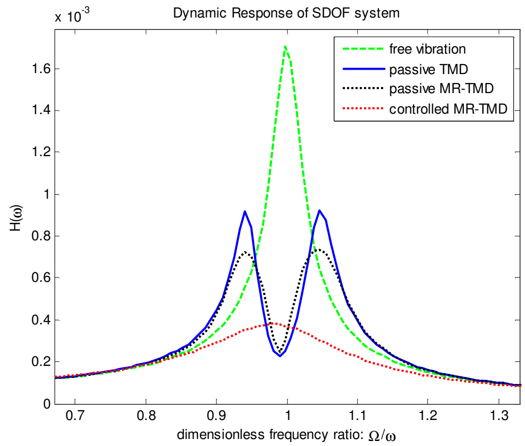

Figure 2: SDOF H(ω).

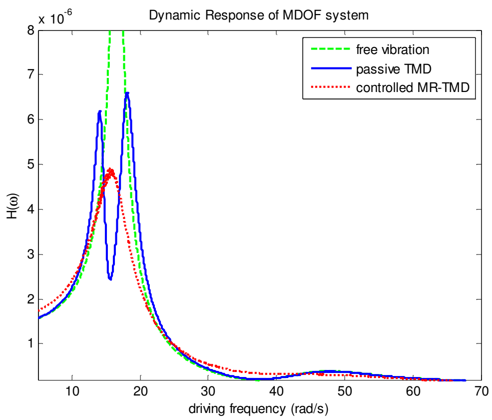

Figure 3: MDOF H(ω).

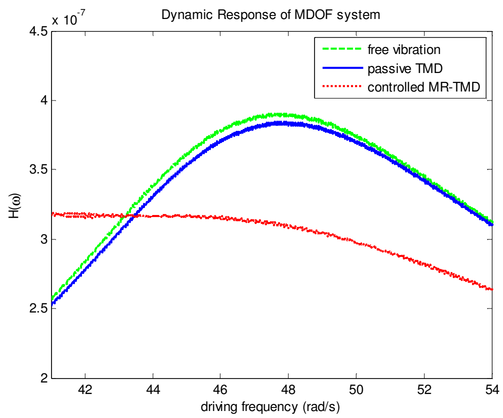

Figure 4: MDOF H(ω) – Second Resonance .

For the 3 DOF system, eigenvalue decomposition shows this system to have resonant frequencies of 16.7, 46.7, and 67.4 rad/s. To cover all relevant frequencies, the dynamic loading sweeps from 0 to 70 rad/s. The passive TMD is tuned to the first mode. As shown in Fig. 3, overall response at the first resonance is attenuated with a frequency range comparable to that of a passive TMD, with slightly improve mitigation results. Highlighting the second resonance, as done in Fig. 4, demonstrates that the controlled MR-TMD is capable of response mitigation for resonances significantly removed from the standard bandwidth of a passive TMD. However, there is a region located on the left-hand side that shows a higher response than the uncontrolled case. It is suspected that the controller could be improved in order to mitigate vibrations in this region. For further analysis, a frequency-shaping controller will be designed and utilized in the simulation.

The frequency range response for Fig. 2 is in agreement with the results of Pinkaew and Fujino [6], who simulated the steady-state frequency responses of a structure under a passive TMD and an idealized STMD with varying c_d. Fig. 3 correlates with the results of [7], where the authors used a similar three-story building to compare the effectiveness of STMD control algorithms. As can be seen in all figures, the controlled MR-TMD improves upon the effectiveness of the passive TMD, except for a small region around the resonance frequency.

REFERENCES

[1] Connor, J. (2003). *Introduction to Structural Motion Control.* Prentice Hall.

[2] Housner, G.W., et al. (1997). Structural Control: Past, Present, and Future. *ASCE J. Eng. Mech*, *123*, 897-971.

[3] Spencer, B. F., & Nagarajajah, S. (2003). State of the Art of Structural Control. *Journal of Structural Engineering* , *129* (7), 845-856.

[4] Wu, J.-C., Lu, W.-C., & Hsu, W.-C. (2006, Januray). Implementation of a Feasible Control Design Process Incorporating Robustness Criteria for Wind-Excited High-Rise Buildings. *Journal of Structural Engineering* , 89-101.

[5] Kim, H., & Adeli, H. (2005, December). Wind-Induced Motion Control of 76-Story Benchmark Building using the Hybrid Damper-TLCD System. *Journal of Structural Engineering* , 1794-1802.

[6] Pinkaew, T., & Fujino, Y. (2001). Effectiveness of Semi-Active Tuned Mass Dampers under Harmonic Excitation. *Engineering Structures*, 23, 850-856.

[7] Lee, C.L. *et al*. (2006). Optimal Design Theories and Applications of Tuned Mass Dampers. *Engineering Structures*, *28*, 43-53.

[8] Lin, P.-Y., & Loh, C.-H. (2008). Semi-Active Control of Floor Isolation Systems using MR-Damper. *Proceedings of SPIE - Sensors and Smart Structures Technologies for Civil, Mechanical and Aerospace Systems , 6932*, 69320U- 1-11.

[9] Ji, H.R., *et al.* (2005). Structural Vibration Control using Semiactive Tuned Mass Damper. *The Eightennth KKCNN Symposium on Civil Engineering, Taiwan.*

[10] Yang, G., Spencer, B. F., Jung, H.-J., & Carlson, J. D. (2004, September). Dynamic Modeling of Large-Scale Magnetorheological Damper Systems for Civil Engineering Applications. *Journal of Engineering Mechanics* , 1107-1114.

[11] Frahm, H. (1911). Device for Damping Fibration of Bodies. U.S. Patent No. 989-958.

[12] Hartog, Den (1940). *Mechanical Vibrations, 1st ed.* NY: McGraw Hill.

[13] Fujino, Y., & Abe, M. (1982). Dynamic Characterization of Multiple Tuned Mass Dampers and Some Design Formulas. *Earthquake Engineering and Structural Dynamics*, *10*, 813-835.

[14] Spencer, B.F., *et al*. (1997). Phenomenorheological Model for Magnetorheological Dampers. *Journal of Engineering Mechanics*, 230-238.

[15] Adhikari, R., & Yamaguchi, H. (1997). Sliding Mode Control of Buildings with ATMD. *Earthquake Engineering and Structural Dynamics , 26*, 409-422.

[16] Dyke, S., Spencer, B., Sain, M., & Carlson, J. (1996). Modeling and Control of Magnetorheological Dampers for Seismic Response Reduction. *Smart Materials and Structures , 5* (5), 565-575.

[17] Utkin, V. I., & Young, K. D. (1978). Methods for Contructing Discontinuous Planes in Multidimensional Variable Structure Systems. *Automation Remote Control , 31*, 1466-1470.

[18] Jansen, L. M., & Dyke, S. J. (2000). Semiactive Control Strategy for MR Dampers: Comparative Study. *Journal of Engineering Mechanics , 126* (8), 795-803.

[19] Yoshida, O., Dyke, S. J., Giacosa, L. M., & Truman, K. Z. (2003). Experimental Verification of Torsional Response Control of Asymetric Buildings using MR Dampers. *Earthquake Engineering and Structural Dynamics , 32* (13), 2085-2105.